Exact Range and Bearing Control of Many Differential-Drive Robots with Uniform Control Inputs

Aaron Becker and James McLurkin

***Abstract*— In this paper we investigate controlling many nonholonomic unicycles that each receive exactly the same inputs. The robots are *almost* homogeneous, but each robot has a unique parameter that scales its turning rate. Previous work showed that such a collection of robots can be approximately steered to arbitrary Cartesian positions, but not to arbitrary heading angles in a global reference frame. We extend this work by proving we can always steer such a collection of robots exactly to arbitrary range and bearing locations relative to targets in $\mathbb{R}^2$ in a finite number of steps. We also provide existence proofs for controlling the final heading angles of many robots. This work addresses a fundamental challenge in micro- and nanorobotics with possible applications in targeted therapy, sensing, and actuation. Scale hardware experiments validate the control policy. All code is provided online.**

I. Introduction

Micro- and nanorobots can be produced in very large numbers. For micro- and nanorobotics, the marginal cost of producing one additional robot is astonishingly small. Micro-robots can be fabricated using MEMS techniques [1], [2], which can be tiled to produce multiple copies at marginal additional cost. Nanocars are exemplary of this diminishing marginal cost. Nanocars are synthetic molecules with integrated axles, rolling wheels, and light-driven motors. These are routinely produced in quantities that are amazing—a batch the size of an aspirin tablet contained $\approx 4 \times 10^{19}$ nanocars [3], [4]. This dwarfs the total number of birds on the planet earth—some 3×10^{11} [5].

While it is now possible to create large populations of micro- and nanorobots, a current bottleneck is control. These systems [1]–[4], [6] all rely on global inputs, where each robot receives an exact copy of the control signal. A reasonable question is "What control inputs will steer many robots simultaneously to goal states?" To answer this question, we focus on systems, including [2]–[4], that can be modeled as nonholonomic unicycles. For a system of n robots, there are $3n$ degrees of freedom, the x, y positions and global headings θ. If the robots have unique turning rates, we provide a finite-time open-loop algorithm to control $2n+1$ degrees of freedom. This limitation does not exclude many useful applications, such as navigation, manipulation, or assembly. In this paper we present two useful ways to allocate these $2n+1$ DOF:

A.) unique (x_i, y_i) positions for each robot with θ_i—the robot heading in a global reference frame—a scaled value of the input mod(2π) and

A. Becker and J. McLurkin are with the Computer Science Department, Rice University, Houston, TX 77005 USA aabecker@gmail.com, jmclurkin@rice.edu

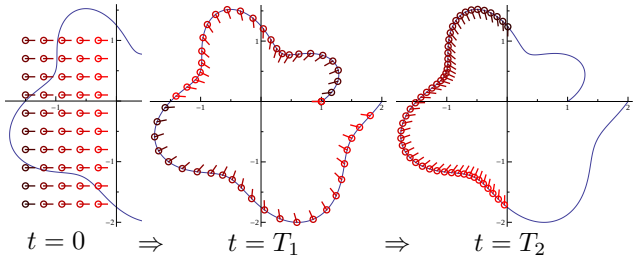

Fig. 1. n robots, under the constraint that each robot receives exactly the same control inputs, can be controlled from any initial configuration to the perimeter of a star-shaped set as long as each robot has a unique turning rate. The controller has $2n+1$ degrees of freedom, which can be used to permute the spacing around the perimeter (middle and right). See Section IV for details.

B.) unique (d_i, α_i) range and bearing to targets for each robot with ψ_i—the bearing from the target to the robot—a scaled function of the input and α_i mod(2π). We focus on this second behavior, which is illustrated in Figs. 1 and 2.

Heading control is necessary for many robotic tasks, including:

1) redirecting an incoming signal (i.e. solar incinerators)
2) observing an object (collecting, measuring, cameras)
3) emitting an object (ballistics, targeted drug therapy)
4) manipulating objects (pushing, grasping)

On the nanoscale, heading control is no less necessary. Possible applications include using molecular robots as nanoscale transporters, for breaking chemical bonds, or for building structures by constructing non-covalent bonds. We derive inspiration from the molecular actuators of Minett et al. [7] and the molecular elevators of Badjíc at al. [8].

Our paper is organized as follows. We begin in Section II with a description of our problem. Section III investigates controlling the heading of an ensemble of robots. In Section IV we design a finite step control law for range and bearing control of a finite ensemble of robots. We discuss the results of simulations and hardware experiments in Section V, and end with concluding remarks in Section VI.

II. An Ensemble of Differential-Drive Robots

Consider a collection of n unicycles that each roll without slipping. Following the terminology of [9], [10], we call this collection an *ensemble* and describe the configuration of the ith robot by $\mathbf{q}_i = [x_i, y_i, \theta_i]^\top$ and its configuration space by $\mathcal{Q} = \mathbb{R}^2 \times \mathbb{S}^1$. The global control inputs are the forward speed $u \in \mathbb{R}$ and turning rate $\omega \in \mathbb{R}$. We assume that each robot has a unique nonzero parameter ϵ_i that scales the turning rate ($|\epsilon_i| \neq |\epsilon_j| \ \forall \ i, j$). These ϵ_i values may arise from stochastic processes during manufacturing [2], or as design decisions

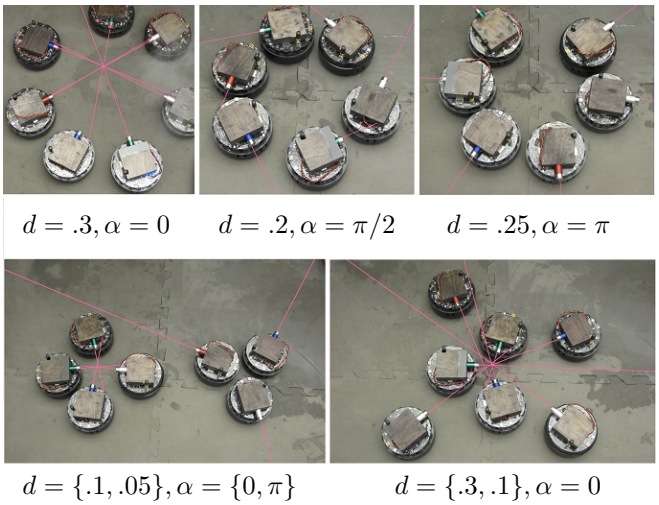

Fig. 2. Differential-drive robots with top-mounted lasers demonstrating our control technique. By selecting different distances d and bearings $\alpha = \{0, \pi/2, \pi\}$, these robots engage, form a perimeter, or protect the target. The second row illustrates how these parameters can be mixed and applied to multiple targets, or to form concentric rings. The robots receive exactly the same control commands, but each robot has a unique turning rate. (See multimedia attachment: http://www.youtube.com/watch?v=4K_OvQqhR6Q)

[11]. The kinematics of the unicycle are given by

$$\dot{\mathbf{q}}_i(t) = u(t) \begin{bmatrix} \cos\theta_i \\ \sin\theta_i \\ 0 \end{bmatrix} + \epsilon_i \omega(t) \begin{bmatrix} 0 \\ 0 \\ 1 \end{bmatrix}. \tag{1}$$

A. Previous Work

Given $\mathbf{q}(0), \mathbf{q}_{\text{goal}} \in \mathcal{Q}$, the control problem for regulating position is to find inputs $u(t)$ and $\omega(t)$ such that for any $\mathbf{q}(0)=[x(0), y(0), \theta(0)]^\intercal$ and $\mathbf{q}_{\text{goal}}=[x_{\text{goal}}, y_{\text{goal}}, \theta_{\text{goal}}]^\intercal$,

$$\lim_{t\to\infty} \left\| \begin{bmatrix} x(t) \\ y(t) \end{bmatrix} - \begin{bmatrix} x_{\text{goal}} \\ y_{\text{goal}} \end{bmatrix} \right\|_2 = 0.$$

In [12] we proved that systems described by (1) can be approximately steered to within a μ-ball of arbitrary positions in $\mathbb{R}^2$. In [13] we provided closed-loop controllers to drive n robots to n target positions. For both works, the control laws apply even to an infinite robot continuum.

Unfortunately, in [12], we proved that the heading angles of the ensemble members—the θ_i values—are not controllable. The final heading of every robot in the ensemble is the scaled integration of all the turning control inputs, i.e. $\theta_i(T) = \theta_i(0) + \epsilon_i \int_0^T \omega(t)\,\mathrm{d}t$. Instead of a full-state controller, we provided a control law that steered the position of each robot's center of rotation.

Our goal is to provide control algorithms for many robots with uniform inputs, with applications in trajectory following, manipulation, force-closure, and assembly at the micro- and nanoscale. Regrettably, being unable to control the heading of the robots makes many tasks difficult or impossible. For instance, manipulation and assembly work without heading control requires that the robots be able to rotate in place and be circular, since we cannot specify the incident angle of the robots.

This paper extends previous work with robot ensembles by controlling the *relative* final heading—the bearing to a fixed target from each robot. To accomplish this, our algorithm exploits the fact that we can precompute the final heading of the robots after applying any input sequence. Additionally, we provide an exact, finite-step control algorithm.

B. Conversion to Discrete-Time

We model our robotic system with a discrete-time model. We can simplify (1) by splitting each ΔT time step into two stages with piecewise constant inputs. During the first stage of round k we command the robots to turn in place ϕ, and during the second stage we command the linear velocity $u(k)$.

$$k = \left\lfloor \frac{t}{\Delta T} \right\rfloor$$
$$\begin{bmatrix} u(t), \omega(t) \end{bmatrix} = \begin{cases} \left[0, \quad \frac{2}{\Delta T}\phi\right] & t - k\Delta T < \frac{\Delta T}{2} \\ \left[\frac{2}{\Delta T}u(k), 0\right] & \text{else} \end{cases} \tag{2}$$

Because the robots are either turning in place or moving in a straight line, we can precompute the heading angles and write the kinematics in the following simple form

$$\begin{bmatrix} x_i(k+1) \\ y_i(k+1) \end{bmatrix} = \begin{bmatrix} x_i(k) \\ y_i(k) \end{bmatrix} + \begin{bmatrix} \cos\left(\theta_i(0) + \epsilon_i k\phi\right) \\ \sin\left(\theta_i(0) + \epsilon_i k\phi\right) \end{bmatrix} u(k), \tag{3}$$

for $i = 1, 2, \ldots, n$ and $k \in \mathbb{Z}$. Eq. (3) is a discrete-time linear time-varying system. As $\Delta T \to 0$, the discrete-time ensemble (3) approaches the continuous-time model (1).

C. Uniform k-Step Controllability

To prove (3) is controllable by (2), we will show the system is **uniformly k-step controllable**. This means that the reachable set after k rounds is the entire state-space [14, chap 25.3]. We redefine the state as $\mathbf{p}_i = [x_i, y_i]^\intercal$, and write (3) in standard notation as

$$\mathbf{p}_i(k+1) = A_i(k)\mathbf{p}_i(k) + B_i(k)u(k). \tag{4}$$

Here $A_i(k)$ is the identity matrix for all i, k. The matrix $B_i(k)$ encodes all heading information and has the form

$$B_i(0) = \begin{bmatrix} \cos(\theta_i(0)) \\ \sin(\theta_i(0)) \end{bmatrix}$$
$$B_i(1) = \begin{bmatrix} \cos(\theta_i(0) + \epsilon_i\phi) \\ \sin(\theta_i(0) + \epsilon_i\phi) \end{bmatrix}$$
$$\vdots$$
$$B_i(k) = \begin{bmatrix} \cos\left(\theta_i(0) + \epsilon_i k\phi\right) \\ \sin\left(\theta_i(0) + \epsilon_i k\phi\right) \end{bmatrix},$$

$$\mathbf{B}_k = \begin{bmatrix} B_1(k) \\ B_2(k) \\ \vdots \\ B_n(k) \end{bmatrix}.$$

We then define the controllability matrix $\mathcal{C}_k$ as

$$\mathcal{C}_k = [\mathbf{B}_0, \mathbf{B}_1, \ldots, \mathbf{B}_{k-1}].$$

The finite ensemble with n robots has $3n$ degrees of freedom, but we can control only $2n + 1$ of these, the x, y positions and the net turning command. To control each robot's x, y position requires $\mathcal{C}_k$ to be rank $2n$. If the ϵ_i values are unique,

the functions $\cos(\epsilon_1\phi), \sin(\epsilon_1\phi), \ldots \cos(\epsilon_n\phi), \sin(\epsilon_n\phi)$ are orthogonal on any closed interval of length 2π. This means there always exists a sequence of ϕ_k values that make $\mathcal{C}_k$ full rank. The parameter ϕ controls the sampling frequency, and must be twice the Nyquist frequency [15], or

$$\phi \leq \frac{\pi}{\max\limits_{i\in[1,n]} \epsilon_i}.$$

Sampling theory also gives a bound on k, the number of samples needed [16, Chapter 5]. In order to differentiate two frequencies ϵ_1 and ϵ_2, we need $k \geq \frac{2\pi}{|\epsilon_1 - \epsilon_2|}$. The bound on k is then given by the minimum separation between ϵ values

$$k \geq \frac{2\pi}{\min\limits_{i\neq j\in[1,n]} |\epsilon_i - \epsilon_j|}.$$

D. k-Step Control Law

We desire the sequence of k control inputs $\mathbf{u}_{[0,\ldots,k-1]}$ that will bring the system to the goal state. If $\mathcal{C}_k$ is full rank and $k > 2n$, the system is underdetermined, with an infinite number of solutions. We choose from these solutions by finding the smallest one. That is, for any starting state $\mathbf{p}_0$ and desired final state $\mathbf{p}_1$, the control sequence is derived by minimizing $\left\|\mathbf{u}_{[0,\ldots,k-1]}\right\|_2$ subject to the constraint $\mathcal{C}_k\mathbf{u}_{[0,\ldots,k-1]} = (\mathbf{p}_1 - \mathbf{p}_0)$. The solution is

$$\mathbf{u}_{[0,\ldots,k-1]} = \mathcal{C}_k^\top(\mathcal{C}_k\mathcal{C}_k^\top)^{-1}(\mathbf{p}_1 - \mathbf{p}_0). \tag{5}$$

In practice, the Moore-Penrose pseudo inverse results in better numerical accuracy than the inverse above [17]. We note that for $k = 2n$, $\mathcal{C}_k$ is almost always ill-conditioned, leading to very large control commands. With evenly distributed ϵ values, best results are obtained for $k \approx 4n$, as shown in Fig. 5. When $\mathcal{C}_k$ is full rank, the robots converge exactly.

E. 2n+1: The Final Degree Of Freedom

Our k-step control law allows us to move the robot exactly to n (x, y) coordinates, leaving us with one additional degree of freedom. This degree of freedom is determined by the ϕ values chosen, and an optional turn at the end. There are several possibilities. We can return the robots to their original heading, Section III discusses controlling the robot's final heading, and in Section IV we use this degree of freedom to control the distribution of robots along the perimeter of star-shaped sets.

III. Controlling Heading

In our previous work with continuum ensembles, we proved the heading of an infinite ensemble is not fully controllable [12]. Even with a finite ensemble of robots, we cannot steer the heading angles to any desired goal heading. We often cannot even achieve exact consensus in heading mod(2π). However, it is possible to achieve *approximate* consensus in heading. Given a $\mu > 0$, there exists a ϕ such that $|\text{mod}(\theta_i, 2\pi) - \phi| < \mu$ for all robot headings θ_i in the ensemble.

A. Exact Heading Consensus—Infinite Ensemble

It is impossible to make a continuum of robots, all initialized at $\theta(0, \epsilon)$, with a continuum of turning rates $\epsilon \in [\epsilon_{min}, \epsilon_{max}], \epsilon_{min} \neq \epsilon_{max}, \epsilon \neq 0$ agree in heading at any angle other than the initial heading. Let $\gamma(T) = \frac{1}{2\pi}\int_0^T \omega(t)\,\mathrm{d}t$. Then the heading of the ensemble parameterized by ϵ at time T is $\epsilon\gamma(T)$, and is spread along a continuum of headings from $\epsilon_{min}\gamma(T)$ to $\epsilon_{max}\gamma(T)$.

B. Exact Heading Consensus—Finite Ensemble

For illustration, consider the hands of a 12-hour clock. The hour and minute hands overlap 22 times per day, every 12/11 hours (the first crossing is at ≈1:05:27), but the hour, minute, and second hands overlap only twice: midnight and noon. This overlap occurs once per Least Common Multiple (LCM) of the periods. The LCM of a set of numbers can be obtained from their prime factorizations if the set is *mutually rational*, e.g. the ratio of any two of the numbers is a rational number [18].

Theorem 1: We cannot always make a finite ensemble with different turning rates exactly agree in heading.

Proof: It is sufficient to provide a counterexample. Consider 3 robots; a, b, c, all with different turning rates, where

- a turns at unit velocity
- b turns at 2·unit velocity
- c turns at e·unit velocity (base of natural logarithm)

If all three unicycles are initialized in same direction and commanded to turn at a fixed turning rate, there does not exist a time when they next align. Here, unicycle heading at time t is $t \cdot 2\pi$, $t \cdot \pi$ and $t \cdot e\pi$. Unicycles a and b coincide infinitely often at $t = k2\pi$ for $k \in \mathbb{Z}$. Robots a, c coincide infinitely often when

$$\text{mod}(t, 2\pi) = \text{mod}(t \cdot e, 2\pi).$$

However, the ensemble a, b, and c only coincides when:

$$\text{mod}(k2\pi, 2\pi) = \text{mod}(k2\pi \cdot e, 2\pi)$$

Per modular arithmetic, we divide by the common term 2π:

$$\text{mod}(k, 1) = \text{mod}(k \cdot e, 1) \Rightarrow 0 = \text{mod}(k \cdot e, 1)$$

This equality only holds when the quantity $k \cdot e \in \mathbb{Z}$ for $k \in \mathbb{Z}$. Since e is an irrational number, this does not occur, because the product of a rational and an irrational number is always an irrational number. ■

C. Approximate Heading Consensus—Finite Ensemble

If the set of turning rates is not mutually rational, we cannot reach an exact solution. Instead we search for an approximate solution. Hurwitz' Theorem [19] tells us that an irrational number ϵ_i has an infinity of rational approximations $\frac{p}{q}$ which satisfy $|\epsilon_i - \frac{p}{q}| < \frac{1}{\sqrt{5}q^2}$. In our application, a finite set of robots with unique turning rates and an error bound $\mu > 0$, we can always find a finite $T > 0$ such that the robots' alignment error is less than μ.

The example robots in Section III-B achieve approximate heading consensus at

μ	10^{-1}	10^{-2}	10^{-3}	10^{-4}	10^{-5}	10^{-6}
$\frac{t}{2\pi}$	1	63	3234	7525	196405	4898913

IV. Range and Bearing Control

We define bearing from a robot to a fixed target as the counter-clockwise angle from the robot's heading to a vector toward the target. Given a desired bearing-angle and a desired target, a finite ensemble of robots can be controlled to the perimeter of any star-shaped set around that target, as shown in Fig. 1. We require a function that maps a robot's global heading θ_i to a position on the perimeter of the star shaped set, and that the robots turn at unique rates.

Fig. 1 provides an example: 50 robots with ϵ values evenly distributed $[\frac{1}{2}, \frac{3}{2}]$ are controlled to the perimeter specified by $d(\psi) = 1 + \frac{\psi + \sin(4\psi)}{2\pi}$, $\psi \in [0, 2\pi]$, with bearing $\alpha = 0$. Because the ϵ_i values are mutually rational, we can achieve exact heading consensus. In this example the robot's headings have a period of 196π. By varying the total commanded turn $\gamma(t)$ we can modify the distribution of robots along the perimeter. Shown are $\gamma(T_1) = 50\pi$ and $\gamma(T_2) = 311$.

While our approach works on arbitrary curves, we will describe the technique by controlling the robots to the perimeter of a circle. A circular configuration best addresses our proposed tasks and the procedure is easy to follow. Given n robots, we can specify the desired bearing α and range d for each robot to at most n targets. Let the pose of the ith robot be $(x_i(k), y_i(k), \theta_i(k))$.

After k moves under the motion model (3), the robot is at heading $\theta_i(k) = \theta_i(0) + \epsilon_i k\phi$. Given d, α, and the ith robot's target at $(x_{t,i}, y_{t,i})$, the desired final position is

$$\begin{bmatrix} x_i(k) \\ y_i(k) \end{bmatrix} = \begin{bmatrix} x_{t,i} \\ y_{t,i} \end{bmatrix} - \begin{bmatrix} \cos(\theta_i(0) + \epsilon_i k\phi + \alpha) \\ \sin(\theta_i(0) + \epsilon_i k\phi + \alpha) \end{bmatrix} d. \quad (6)$$

This control enables a host of configurations. Several of these are illustrated in Fig. 3. They include:

1) surrounding the target: by choosing $d = const$ and $\alpha = 0$, the robots will finish all on a circle of radius d centered around and aimed toward the target. This configuration is suitable for monitoring a target or delivering material.

2) aligning around the target: by choosing $d = const$ and $\alpha = \pi/2$, the robots will form up tangent to a circle of radius d. By proper choice of ϕ and k, these robots can be distributed along the perimeter to form a barrier around the target. This may also be a starting point for caging manipulation (Kumar [20]).

3) defending the target: by choosing $d = const$ and $\alpha = \pi$, the robots will form up in a circle of radius d pointing away from the target.

4) mixing configurations: up to n targets may be specified for the n robots, and each robot can be given particular values of (d, α). This may be used to surround multiple targets, form multiple layers around certain targets, or track multiple targets.

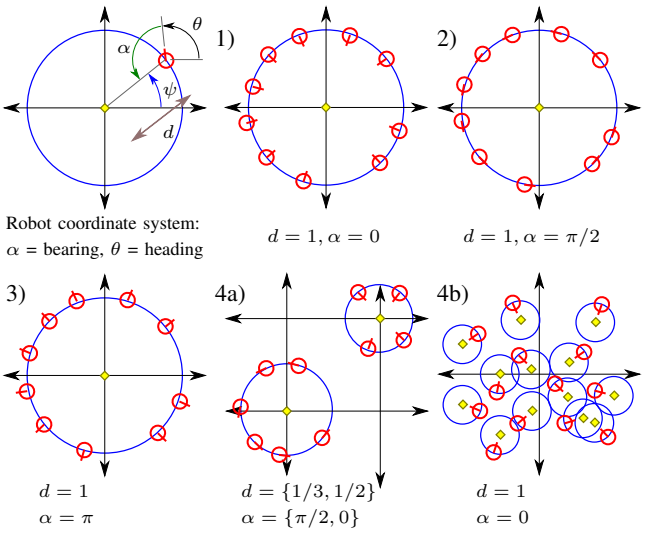

Fig. 3. Given n robots, where the pose of the ith robot is (x_i, y_i, θ_i), we can specify the desired bearing α and range d for each robot to at most n targets at positions (x_{ti}, y_{ti}). Let $\psi = \text{atan2}(x_i - x_{t,i}, y_i - y_{t,i})$, then the heading $\theta = \pi - \alpha + \psi$.

A. Human Control of Ensembles

Our preliminary experiments raise intriguing questions about human control of multiple robots [21] and what type of user interaction is most appropriate. Our interest in potential applications in micro- and nanorobotics led us to produce a game version. In this game, the user attempts to drive n remote control robots, each equipped with suction-cup darts, within a specified distance of an unwary target. The user is scored based on the number of darts that reach the target. The game is available online [22] and is surprisingly difficult, even for low values of n. Future work will investigate what level of supervisory control is most appropriate.

V. Results

A. Simulations

We examine the dependence of overall path length on the number of robots n and the number of moves k. This allows us to predict the number of moves necessary to move an ensemble of robots from start to goal configurations with a near-optimal path length. We desire short paths because under open-loop control, the true state diverges from the predicted state due to process noise. This noise is a function of the input commands, distance travelled, and modeling errors [23]. To minimize state error we want to create short paths with few turns.

Each simulation starts with the ensemble of n robots initialized evenly spread with $x = 0$ and $y \in [-1, 1]$. The target is at (2,0), the commanded turn at each step $\phi = \pi/4$, and the desired range and bearing to the target is $(d, \alpha) = (1, 0)$. This setup with solutions for $k = 70$ and 500 is shown in Fig. 4.

We investigated path length as a function of number of moves k for $k = [1, 500]$, and ran simulations for $n = \{2, 5, 10, 20, 35, 50, 75, 100\}$. By assigning a turning cost of 1/10 for each turn of $\phi = \pi/4$, which approximates the total distance moved for a similar turn on our hardware robots,

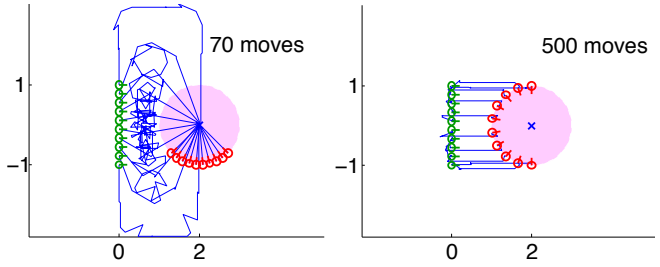

Fig. 4. Simulation set up. The n robots are initialized evenly spread between $y = [-1, 1]$, the goal is at (2,0), the nominal turn $\phi = \pi/4$, and the desired range and bearing to the target is $(d, \alpha) = (1, 0)$. Shown above are results for $n = 10$ robots for different numbers of moves.

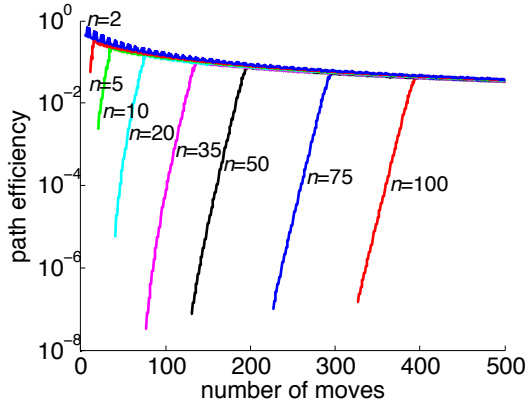

Fig. 5. Semi-log plot of path efficiency (7) as a function of the number of moves allowed for the control law (5). Results are shown for different numbers of robots n. The same initial and target distributions are used for each test, as shown in Fig. 4. All solutions bring the robots exactly to the goal position, but increasing the number of moves helps initially. The paths increase in efficiency until $\approx 4n$ as $\mathcal{C}_k$ becomes well conditioned, then decrease as the cost of turning dominates.

we calculated the path length as

$$\text{path length} = k\frac{1}{10} + \sum_{1}^{k} |u| \,.$$

To facilitate comparison, we compare using the nondimensionalized quantity

$$\text{path efficiency} = \frac{1}{n}\sum_{i=1}^{n} \frac{\text{path length}}{\text{distance}(robot_i, goal)}. \qquad (7)$$

The results of these tests are shown in Fig. 5. Note that when the number of moves is less than $\approx 2n$, the matrix $\mathcal{C}_k$ is not invertible. The paths increase in efficiency from $k = 2n$ to about $k = 4n$ as $\mathcal{C}_k$ becomes well conditioned, then decrease as the cost of turning dominates.

Using the same initial setup, we examined the probability of collision as a function of (robot diameter/mean distance to goal) and the number of robots. We ran simulations for $n = \{2, 5, 10, 20\}$ robots with radius values ranging from 0.001 to 0.1 units. For each radius and number of robots, we ran 100 tests by varying the turning ϕ values and number of moves k. In these tests, we checked the generated path for inter-robot collision.

$$\text{Probability of collision} = \frac{\text{tests with collision}}{100}$$

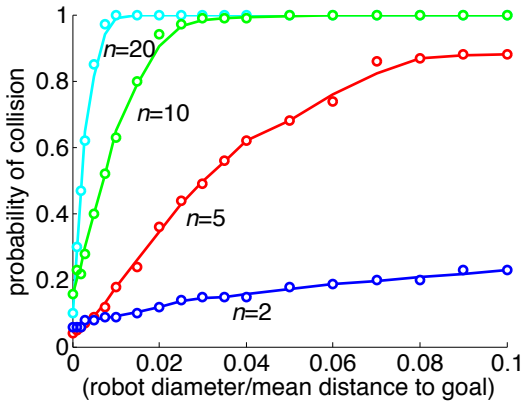

Fig. 6. Probability of a collision as a function of (robot diameter/mean distance to goal) for different numbers of robots, n. The setup in Fig. 4 is used. The probability of collision increases nonlinearly with number of robots and robot radius.

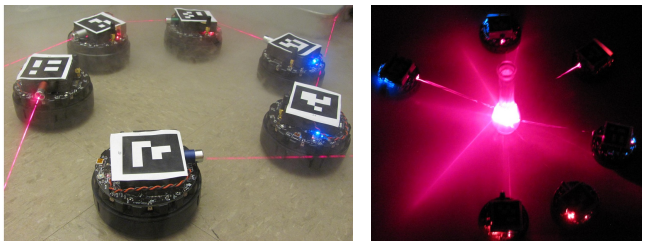

Fig. 7. The r-one robots used for hardware verification (10 cm diameter robots). Each robot carries a laser-pointer for visualizing heading. The top-mounted AprilTag fiducial [25] is used for ground truth measurements. Broadcast radio commands are sent simultaneously to all robots. See multimedia attachment.

The results of these tests are shown in Fig. 6. The probability of collision increases nonlinearly with number of robots and robot radius. The probability that at any time, n randomly distributed robots collide grows quadratically in n. These results indicate that collisions provide a hard-limit on open-loop control for high robot densities.

B. Hardware Experiments

Our differential robots [24] have two direct-drive wheels, and a ball caster in the back, as shown in Fig. 7. These robots are circular and can turn in place. Each robot is given a unique internal parameter ϵ_i that scales turning rate, $\epsilon_i \in [\frac{1}{2}, \frac{3}{2}]$. AprilTag fiducials [25] are mounted on the top of each robot and used to track robot pose. Each robot carries a laser-pointer to easily visualize the heading. We calibrated one robot using the UMBmark routine [26], then stored a unique turning rate ϵ on each robot.

For our experiments we used three r-one robots. These robots were commanded to engage a target located at (1.2,1.2) m with a desired bearing of $\alpha = \pi$ and $d = 0.3$ m. Turning rates are evenly distributed in $[\frac{1}{2}, \frac{3}{2}]$, and the initial robot positions are distributed on $x = [0, 0.2]$ m. The results of 10 hardware experiments are shown in Fig. 8. The attached video includes one experimental run. The final positions had an average distance error of 4.4 cm with standard deviation 2.8 cm and average heading error of 0.13 radians with

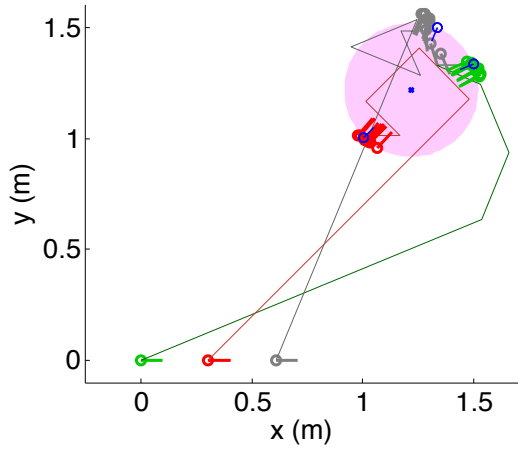

Fig. 8. Hardware results. Three robots are commanded to engage a target (a desired bearing of $\alpha = \pi$ and $d = 0.3$ m). The target is represented by the magenta disc centered around a blue 'x' at (1.2,1.2) m. Turning rates were evenly distributed in $[\frac{1}{2}, \frac{3}{2}]$, and the initial robot positions are distributed on $x = [0, 0.2]$ m. The commanded robot paths are shown in three colors, as are the final positions for 10 hardware experiments. The expected final positions are drawn in blue. The attached video includes one experimental run.

standard deviation 0.20 radians. These small errors appear to be due to wheel slip and are within our calibration accuracy.

VI. Conclusion

In this paper we examined heading control of an ensemble of nonholonomic unicycles. We provided a control policy to steer n robots with unique turning rates to desired range and bearing values in a finite number of steps. This control policy was validated in simulation and in hardware experiments.

There are several limitations to this work. Our current control law is open-loop. Unfortunately, pose estimation error from dead-reckoning increases with path length. The path length for our control law increases with the number of robots (Fig. 5). This restricts our current control solution to systems with excellent odometry or low numbers of robots.

Another problem is due to robot collisions. Collisions corrupt dead-reckoning position and may prevent robots from reaching their goal positions. The control law (5) does not account for collisions. The probability of collision increases with the square of the number of robots. One method to mitigate this is to wrap (5) in a loop and check for collisions along the path. If collisions are found, new values for the turn command ϕ and the number of moves m are tried until a collision-free path is discovered or the maximum number of trials is reached. We provide code implementing this scheme in MATLAB as a free download [22].

Both problems could be alleviated by a closed-loop controller. This control strategy might derive inspiration from existing bearing controllers such as that of Wei et al. [27], or the closed-loop ensemble controllers in [13] and [28].

VII. Acknowledgements

The authors thank Nelson Chen and Quillan Kaseman for assistance with the hardware experiments. We also thank Bill Amend, whose light-hearted Sunday comic of 1/8/2012 inspired us. This work was supported by the National Science Foundation under CPS-1035716.

References

[1] S. Tottori, L. Zhang, F. Qiu, K. Krawczyk, A. Franco-Obregón, and B. J. Nelson, "Magnetic helical micromachines: Fabrication, controlled swimming, and cargo transport," *Advanced Materials*, vol. 24, no. 811, 2012.

[2] B. Donald, C. Levey, and I. Paprotny, "Planar microassembly by parallel actuation of MEMS microrobots," *J. of MEMS*, vol. 17, no. 4, pp. 789–808, Aug. 2008.

[3] Y. Shirai, A. J. Osgood, Y. Zhao, K. F. Kelly, and J. M. Tour, "Directional control in thermally driven single-molecule nanocars," *Nano Letters*, vol. 5, no. 11, pp. 2330–2334, Feb. 2005.

[4] P.-T. Chiang, J. Mielke, J. Godoy, J. M. Guerrero, L. B. Alemany, C. J. Villagómez, A. Saywell, L. Grill, and J. M. Tour, "Toward a light-driven motorized nanocar: Synthesis and initial imaging of single molecules," *ACS Nano*, vol. 6, no. 1, pp. 592–597, Feb. 2011.

[5] K. J. Gaston and T. M. Blackburn, "How many birds are there?" *Biodiversity and Conservation*, vol. 6, no. 4, pp. 615–625, 1997-04-01.

[6] P. Vartholomeos, M. Akhavan-Sharif, and P. E. Dupont, "Motion planning for multiple millimeter-scale magnetic capsules in a fluid environment," in *IEEE Int. Conf. Rob. Aut.*, May 2012, pp. 1927–1932.

[7] A. Minett, J. Fràysse, G. Gang, G. Kim, and S. Roth, "Nanotube actuators for nanomechanics," *Current Applied Physics*, vol. 2, no. 1, pp. 61–64

[8] J. Badjić, V. Balzani, A. Credi, S. Silvi, and J. Stoddart, "A molecular elevator," *Science*, vol. 303, no. 5665, pp. 1845–1849 2004.

[9] R. W. Brockett and N. Khaneja, "On the control of quantum ensembles," in *System Theory: Modeling, Analysis and Control*, T. Djaferis and I. Schick, Eds. Kluwer Academic Publishers, 1999.

[10] J.-S. Li and N. Khaneja, "Ensemble control of Bloch equations," *IEEE Trans. Autom. Control*, vol. 54, no. 3, pp. 528–536, Mar. 2009.

[11] K. E. Peyer, L. Zhang, and B. J. Nelson, "Bio-inspired magnetic swimming microrobots for biomedical applications," *Nanoscale*, 2013.

[12] A. Becker and T. Bretl, "Approximate steering of a unicycle under bounded model perturbation using ensemble control," *IEEE Trans. Robot.*, vol. 28, no. 3, pp. 580–591, Jun. 2012.

[13] A. Becker, C. Onyuksel, and T. Bretl, "Feedback control of many differential-drive robots with uniform control inputs," in *IEEE Int. Rob. and Sys.*, Oct. 2012.

[14] W. S. Levine, Ed., *The Control Handbook*. United States of America: CRC Press, Inc., 1996, ch. 25.3 Discrete-Time Linear Time-Varying Systems, pp. 459–463.

[15] C. E. Shannon, "Communication in the presence of noise," *Proc. Institute of Radio Engineers, Reprint as classic paper in: Proc. IEEE, vol. 86, no. 2, (Feb. 1998)*, vol. 37, no. 1, pp. 10–21, Jan. 1949.

[16] J. G. Proakis and D. G. Manolakis, *Digital signal processing: principles, algorithms, and applications*. Englewood Cliffs, NJ: Prentice Hall, 1996.

[17] R. Penrose, "A generalized inverse for matrices," *Proc. Cambridge Phil. Soc.*, vol. 51, pp. 406–413, 1955.

[18] R. L. Graham, D. E. Knuth, and O. Patashnik, *Concrete Mathematics: A Foundation for Computer Science*. Reading, MA: Addison-Wesley, 1990.

[19] K. Chandrasekharan, *An Introduction to Analytic Number Theory*. Berlin: Springer-Verlag, 1968, p. 23.

[20] J. Fink, N. Michael, and V. Kumar, "Composition of vector fields for multi-robot manipulation via caging," in *Robotics Science and Systems*, Atlanta, GA, Jun. 2007.

[21] D. R. Olsen Jr and S. B. Wood, "Fan-out: Measuring human control of multiple robots," in *SIGCHI Conference on Human Factors in Computing Systems*, Vienna, Austria, Apr. 2004, pp. 231–238.

[22] A. Becker. (2012, Sep.) "Range and Bearing Control of an Ensemble of Robots". [Online]. Available: http://www.mathworks.com/matlabcentral/fileexchange/38190

[23] Y. Zhou and G. Chirikjian, "Probabilistic models of dead-reckoning error in nonholonomic mobile robots," in *IEEE Int. Conf. Rob. Aut.*, vol. 2, Sep. 2003, pp. 1594–1599.

[24] J. McLurkin, A. Lynch, S. Rixner, T. Barr, A. Chou, K. Foster, and S. Bilstein, "A low-cost multi-robot system for research, teaching, and outreach," *Distributed Autonomous Robotic Systems*, pp. 597–609, 2010.

[25] E. Olson, "AprilTag: A robust and flexible visual fiducial system," in *IEEE Int. Conf. Rob. Aut.* IEEE, May 2011, pp. 3400–3407.

[26] J. Borenstein and L. Feng, "Measurement and correction of systematic odometry errors in mobile robots," *IEEE Trans. Robot. Autom.*, vol. 12, no. 6, pp. 869–880, Dec 1996.

[27] R. Wei, R. Mahony, and D. Austin, "A bearing-only control law for stable docking of unicycles," in *IEEE Int. Rob. and Sys.*, vol. 4, Oct. 2003, pp. 3793–3798.

[28] K. Beauchard, J.-M. Coron, and P. Rouchon, "Controllability issues for continuous-spectrum systems and ensemble controllability of Bloch equations," *Comm. Math. Phys.*, vol. 296, no. 2, pp. 525–557, Jun. 2010.